Energy exchange dynamics of the discrete nonlinear Schrödinger equation lattice and intrinsic formation of strongly localized states

D. Hennig
Fachbereich Physik, Freie Universität Berlin, Institut für Theoretische Physik, Arnimallee 14, 14195 Berlin, Germany
(Received 6 November 1996; revised manuscript received 20 March 1997)

We study the dynamics of excitation energy transfer along a lattice chain modeled by the discrete nonlinear Schrödinger (DNLS) equation. We prove that a segment carrying resonant motion can be decoupled from the remainder of the chain supporting quasiperiodic dynamics. The resonant segment from the extended chain is taken to be a four-site element, viz., a tetramer. First, we focus interest on the energy exchange dynamics along the tetramer viewed as two weakly coupled DNLS dimers. Hamiltonian methods are used to investigate the phase-space dynamics. We pay special attention to the role of the diffusion of the action variables inside resonance layers for the energy migration. When distributing the energy initially equally between the two dimers one observes a directed irreversible flow of energy from one dimer into the other assisted by action diffusion. Eventually on one dimer a stable self-trapped excitation of large amplitude forms at a single site while the other dimer exhibits equal energy partition over its two sites. Finally, we study the formation of localized structure on an extended DNLS lattice chain. In particular we explore the stability of the so-called even-parity and odd-parity localized modes, respectively, and explain their different stability properties by means of phase-space dynamics. The global instability of the even-parity mode is shown. For the excited even-parity mode a symmetry-breaking perturbation of the pattern leads to an intrinsic collapse of the even-parity mode to the odd-parity one. The latter remains stable with respect to symmetry-breaking perturbations. In this way we demonstrate that the favored stable localized states for the DNLS lattice chain correspond to one-site localized excitations. [S1063-651X(97)09108-3]

PACS number(s): 63.20.Pw, 03.40.Kf, 63.20.Ry

I. INTRODUCTION

In this paper we study the energy transfer on a nonlinear one-dimensional lattice described by the discrete nonlinear Schrödinger (DNLS) equation

$$i\frac{dc_n}{dt}=\gamma|c_n|^2c_n+V(c_{n+1}+c_{n-1}), \tag{1}$$

where the c_n are complex amplitudes at site n, γ is the local nonlinearity parameter, and V is the dispersion parameter determining the linear coupling between the sites. Equation (1) is also known as the discrete self-trapping (DST) system and presents a set of coupled nonlinear classical oscillators, introduced by Eilbeck, Lomdahl, and Scott [1] as a model to describe the nonlinear vibrational dynamics in small polyatomic aggregates. The DST system can also be applied to model the self-trapping phenomena in chemical, condensed matter, and optical systems [2]. Another motivation for DST studies was to investigate the self-trapping of vibrational energy in larger systems modeling globular protein chains or crystalline acetanilide [3,4].

Equation (1) arises furthermore as a discretization of the continuum nonlinear Schrödinger (NLS) equation. The latter is completely integrable [5,6] and possesses soliton solutions that play an important role in a large number of physical and mathematical problems. However, the application of continuum equations disregarding the inherent discrete lattice structure of the system is often too idealized and gives appropriate results only if the spatial extension of the nonlinear wave is much larger than the lattice spacing so that discretized equations provide suitable descriptions. Unfortunately, there are only a few examples of exactly solvable discrete lattices known, such as the Toda lattice [7] and the Ablowitz-Ladik lattice [8], and most nonlinear lattice systems are nonintegrable. In fact, numerical studies of the dynamics of the discrete version of the NLS equation in the form of the DNLS equation (1) exhibit nonintegrability (see, e.g., [9,10]). Hence, in this case the discreteness not only breaks the continuous translational symmetry, but it destroys at the same time the integrability. The question is then: What becomes of the exact soliton solutions of the integrable NLS equation under the influence of discreteness effects? For the DNLS equation the existence of a localized state with frequency lying below the linear phonon band was established [11,12]. This solitarylike state reduces to a one-soliton solution in the continuum NLS equation. However, in the DNLS equation a moving localized state experiences dispersion and eventually decays [10,11]. Nevertheless, the lack of integrability in the DNLS equation does not necessarily lead to the absence of (standing) localized states at all. It is rather so that large amplitude solitarylike standing excitations in nonintegrable systems appear as well [13] and modulational instability generates a possible mechanism for the intrinsic collapse to such very localized self-trapped states [14,15].

Recently in studies of nonlinear Hamiltonian lattices there has arisen interest in breather solutions, which are time-oscillating solutions whose amplitudes decay exponentially in space [16–29]. The DNLS equation represents such a nonlinear network that can be cast in a Hamiltonian framework. The Hamiltonian is determined by

$$H=\frac{\gamma}{2}\sum_n |c_n|^4+V\sum_n (c_{n+1}^*c_n+c_{n+1}c_n^*) \tag{2}$$

and the equations of motion are obtained through $i dc_n/dt = \partial H/\partial c_n^*$.

For other one-dimensional nonlinear Hamiltonian lattices, such as a chain of particles interacting through harmonic and (quartic) anharmonic potentials, basically two different types of intrinsic localized breathing modes $u_n(t) = \phi_n \cos(\omega t)$ have been observed: These are the so-called even-parity and odd-parity modes, respectively. The odd-parity mode was proposed by Sievers and Takeno [17]. Its spatial amplitudes ϕ_n follow the approximate excitation pattern of $(\ldots \downarrow \uparrow \downarrow \ldots)$. The excitation is localized on only three adjacent lattice sites [17]. The dots stand for vanishingly small amplitudes of the lattice oscillators apart from the three-site excitation peak. Page detected the even-parity mode with spatial pattern $(\ldots \uparrow \downarrow \uparrow \downarrow \ldots)$ where effectively four sites are involved [18]. The odd-parity mode is centered at a lattice site whereas the even-parity mode is centered between two lattice sites. It was shown that the odd-parity mode is unstable with respect to perturbations, whereas the even-parity mode sustains perturbations [30]. Therefore, an interesting question arises, namely, whether one finds these types of localized breathing modes in the DNLS equation as well and if so what stability properties do they have then? The present paper is aimed at offering an answer to these questions in investigating the phase-space dynamics.

To study the breatherlike solutions of the DNLS equation with emphasis on their formation process and stability issues we proceed in the following way: First we use a ''truncation'' argument permitting us to restrict the dynamical studies to only a finite segment of the (infinitely) extended lattice. The truncation is based on the assumption of exponential localization of the major part of the lattice energy on a few lattice elements. Due to the exponential decay of the excitation amplitudes with increasing distance from the highly excited lattice segment those oscillators sufficiently far away from it perform only negligible small-amplitude oscillations not contributing significantly to the lattice energy. Therefore, we are justified in truncating the lattice at a certain lattice point and disregard the dynamics of all oscillators beyond that point. The appropriate length of the truncated chain depends of course on the degree of the exponential localization. Led by the numerical findings for the localized modes of earlier works [21,31,32], a truncation to a four-element segment suffices. For instance, Aceves *et al.* showed that the preferred stable stationary states of the DNLS equation are supported by excitation patterns with energy in only a few lattice sites [31,32]. They also showed that very confined localized states virtually do not interact with their adjacent sites. As we will demonstrate in the first part of the paper the four-mode approximation will give us valuable information about what type of lasting stable localized solution we can expect to find for the DNLS equation at all. Local phase-space approaches were successfully applied to the dynamics of Fermi-Pasta-Ulam chains as well as nonlinear Klein-Gordon chains in [22] and to weakly coupled rotators in [33]. In Sec. II we give a rigorous justification of the truncation of a finite segment supporting periodic motion from the full lattice in the light of classical perturbation theory. The remaining part of the paper is then organized as follows. In Sec. III we study a DNLS tetramer. Using a symmetry-reduction method, we reduce the dynamical problem to a three degree of freedom (DOF) Hamiltonian system. We show that for certain initial conditions the tetramer dynamics can be solved exactly. In Sec. IV the energy migration between the weakly coupled dimers manifested by diffusion of an action variable inside layers of coupled resonances in the underlying phase space is analyzed. Section V is devoted to an investigation of the stability issue of two kinds of localized DNLS modes, namely, the odd-parity mode and the even-parity mode. Making use of a local phase-space approach, we interpret the stability properties of the tetramer and trimer segments in the context of localized modes on segments embedded in extended chains. We demonstrate the global instability of the even-parity mode with respect to symmetry-breaking perturbations. Moreover, we show that under perturbation the even-parity mode collapses to the odd-parity one. Finally, in Sec. VI we give a summary.

II. DECOUPLING OF A RESONANT SEGMENT

The aim of the present section is to show how a finite number of neighboring rotators with motion near resonances can be decoupled from the whole DNLS lattice of weakly coupled rotators. The perturbation method used here was introduced by Benettin *et al.* in [33,34]. These authors found for a chain of weakly coupled rotators (a simpler model than the DNLS chain) that if the initial conditions of the system are such that some of the rotators are in resonance with their neighbors, then the motion of those rotators has very little effect on the remainder of the system. In other words, the short-range interactions of the resonant part are localized in those regions where the initial conditions are resonant, whereas the nonresonant interaction part is very small. Hence all the observed dynamics have local character and in [34] some sort of local chaos as well as local ordered regimes were observed in the resonant regions. In the present study we deal with the case of an arbitrarily large lattice of length $1 \leqslant n \leqslant N$ and perform the perturbative computations to first order in ϵ.

In classical first-order perturbation theory one searches for a canonical transformation from the original action-angle variables (J, θ) to new ones $(\overline{J, \theta})$ such that the original Hamiltonian $H = H_0(J) + \epsilon H_1(J, \theta)$ is transformed to a Hamiltonian where the angle variables have been eliminated up to $O(\epsilon)$, i.e.,

$$H^{(1)}(\overline{J, \theta}) = H_0^{(1)}(\overline{J}) + \epsilon^2 H_1^{(1)}(\overline{J, \theta}). \tag{3}$$

Substituting $c_n = \sqrt{J_n}\, \exp(-i\theta_n)$, the DNLS system (2) is brought into the form

$$H = \frac{\gamma}{2} \sum_n J_n^2 + \epsilon 2V \sum_n \sqrt{J_n J_{n-1}}\, \cos(\theta_n - \theta_{n-1})$$
$$\equiv H_0(J) + \epsilon H_1(J, \theta). \tag{4}$$

For a perturbational treatment we consider small couplings V, which we make explicit by introducing the parameter $0 < \epsilon \ll 1$ in front of the coupling terms. Physically, a small V means, for quasiparticles along molecular chains (e.g., in the Holstein model) a small intersite transfer matrix element.

In the studies of molecular aggregates the insertion of spacer molecules increases the intersite distances and lowers the excitonic transfer matrix elements (see, e.g., [35,36]) and thus it is justified to regard the couplings as weak. Furthermore, for a large class of organic systems, such as formamide and dichloromethane, as well as biological macromolecules and crystalline acetanilide as a model of α-helix protein the intermolecular coupling V is small, typically of the order of 8–14 cm^{-1} compared to the local excitation energy carried by the molecular units, which is in the range between 1000 and 2000 cm^{-1} [37].

Finally, also certain electrical lattices built up from coupled cells of nonlinear circuits can be modeled by a DNLS equation [28]. Neighboring cells are bridged via series of linear conductances that can be assigned such that the intercell coupling V becomes small.

In the following we apply the Lie method (see, e.g., [38]) to eliminate the angle variables at first order in perturbation theory. To this end one determines a generating function $S=\epsilon\eta$ of a canonical transformation such that the new Hamiltonian $SH=\exp[\epsilon L_\eta]$ takes the form $H\to H_0^{(1)}+\epsilon^2 H_1^{(1)}+\cdots$ and $L_H f=\{H,f\}$ is determined via the Poisson bracket. One obtains $\exp[\epsilon L_\eta](H_0+\epsilon H_1)=H_0+\epsilon(L_\eta H_0+H_1)+O(\epsilon^2)$. With the relation $L_\eta H_0=-L_{H_0}\eta$ one arrives finally at the equation $L_{H_0}\eta=H_1$ for the unknown function η. Using Eq. (4) one finds

$$\eta(J,\theta)=2V\sum_n \frac{\sqrt{J_n J_{n-1}}}{J_n-J_{n-1}}\sin(\theta_n-\theta_{n-1}). \tag{5}$$

Finally, we discuss the definition of the domains of the canonical transformation $S=\epsilon\eta$. The generating function η is defined outside the resonant planes of $J_n-J_{n-1}=0$ and the condition of nonresonance is fulfilled for $|J_n-J_{n-1}|>4\sqrt{\epsilon VP}$. We use that $J_n\leqslant\sqrt{P}$, where $P=\Sigma_n J_n$ is a conserved quantity.

On the other hand, if on a certain segment of the lattice of rotators the nonresonance conditions cannot be satisfied, that is, if $|J_n-J_{n-1}|<4\sqrt{\epsilon VP}$ for $n\in[N_-^{res},N_+^{res}]$ and $1<N_\pm^{res}<N$, then one can still perform a canonical transformation S to eliminate the angle variables on all lattice points contained in the intervals $n\in[1,N_-^{res}-1]\cup[N_+^{res}+1,N]$. The new Hamiltonian then reads

$$H_0^{(1)}=\frac{\gamma}{2}\sum_{n=1}^{N} J_n^2+\epsilon 2V\sum_{n=N_-^{res}}^{N_+^{res}}\sqrt{J_n J_{n-1}}\cos(\theta_n-\theta_{n-1})+O(\epsilon^2). \tag{6}$$

In this way one decouples a resonant segment of length $\widetilde{N}=N_+^{res}-N_-^{res}$ from the rest of the lattice chain and the energy should stay at this truncated segment at least up to times of order $1/\epsilon$. In the next section we regard the DNLS tetramer of $\widetilde{N}=4$ as the truncated segment.

III. THE DNLS TETRAMER

In the present section we study the DNLS tetramer. The aim of such a study is twofold. The tetramer in itself is interesting with respect to applications, e.g., to energy transfer in molecular aggregates as well as to four-mode coupled optical waveguides.

First, the tetramer can be viewed as a finite segment embedded in an extended chain. The tetramer study serves then as a truncated four-mode description of the infinite lattice dynamics. In particular, there is the relation to the even-parity localized mode. This strongly localized mode involves *only four adjacent particles* (oscillators) of the chain and the rest of the chain is literally at rest and hence can be discarded [13]. It has been shown above rigorously that finite elements carrying resonant motion can be decoupled from the remainder of the chain. We will see that localized tetramer modes can actually be associated with resonances. The question is then: What are the stable localized modes provided by the tetramer and do they persist as strongly localized modes of the extended DNLS chain?

Second, the four-element DNLS segment (tetramer) is the shortest segment for which the dimensionality of the phase space supports the existence of a type of dynamics for which the trajectories can wander freely in phase space known also as Arnold diffusion [39]. As a result of the study on the DNLS energy exchange dynamics, the Arnold diffusion is crucial for driving the transition of the even-parity mode to the odd-parity one to create a stable localized mode (see Sec. IV).

A. Coupled dimers and symmetry reduction

We write the DNLS-tetramer Hamiltonian in terms of the complex site amplitudes as

$$H=\frac{1}{2}\gamma\sum_{j=1}^{4}|c_j|^4+V(c_1^*c_2+c_2^*c_1)+V(c_3^*c_4+c_4^*c_3)+W(c_2^*c_3+c_3^*c_2). \tag{7}$$

We call the pair of lattice sites (1,2) the *first dimer*, while the pair (3,4) constitutes the *second dimer*. Sometimes we refer to them also as dimer 1 and 2, respectively. The choice of different couplings V of the transfer on the dimers respectively between them via W enables us two consider different situations dependent on the relative ratio of V and W. For example; in the case of $V\gg W$ one has two weakly bound dimers. The opposite extreme case of $W\gg V$ is a dimer with one oscillator weakly attached to either site of it.

The system obtained by setting $W=0$ $(V=0)$ is integrable since it decomposes into two integrable DNLS dimers (one dimer and two isolated oscillators). Instead of explicitly writing the equations of motion for the amplitudes c_j of the system, in which, besides energy conservation, the norm $P=\Sigma_{j=1}^4|c_j|^2$ is a further conserved quantity, we first express the Hamiltonian (7) in a different form resulting from a symplectic transformation of the dimer amplitudes to two pairs of canonically conjugate variables (p_n,ϕ_n) and (N_n,β_n), with $n=1,2$:

$$c_1^{(n)}=\sqrt{\frac{N_n+p_n}{2}}\exp\left[-i\left(\frac{\phi_n+\beta_n}{2}\right)\right],$$

$$c_2^{(n)}=\sqrt{\frac{N_n-p_n}{2}}\exp\left[i\left(\frac{\phi_n-\beta_n}{2}\right)\right]. \tag{8}$$

The momentum variables $p_{1,2}$ are equal to the occupation differences between the two sites on each dimer, i.e., $p_n=|c_1^{(n)}|^2-|c_2^{(n)}|^2$. The auxiliary action variables N_n are given by $N_n=|c_1^{(n)}|^2+|c_2^{(n)}|^2$. Obviously, they specify the amount of P contained in each of the dimers, with $P=N_1+N_2$.

It is convenient to rescale the time according to $2Vt\rightarrow\tilde{t}$, which is equivalent to a measurement of the energy in units of $2V$. Thereby we divide the Hamiltonian (energy) by a factor of $2V$ yielding the scaled parameters $\gamma/2V=\tilde{\gamma}$ and $W/V=\tilde{W}$. For the sake of simplicity of notation we omit the tildes henceforth.

The Hamiltonian (7) expressed in these new variables becomes

$$H=H_1^0+H_2^0+H^1, \tag{9}$$

with the dimer parts

$$H_n^0=\frac{\gamma}{2}[N_n^2+p_n^2]+\sqrt{N_n^2-p_n^2}\,\cos\phi_n \quad (n=1,2) \tag{10}$$

and the interaction part

$$H^1=W\sqrt{(N_1-p_1)(N_2+p_2)}\cos[\tfrac{1}{2}(\beta_1-\beta_2)-\tfrac{1}{2}(\phi_1+\phi_2)]. \tag{11}$$

A reduction of the dimensionality of the phase space corresponding to the system of Hamiltonian (9) is possible by applying the symmetry-reduction method [38]. Apparently, the interaction Hamiltonian depends on the angle variables β_n $(n=1,2)$ only in their combination $\beta_1-\beta_2$. The corresponding conserved quantity related to the S^1 symmetry is the integral $P=N_1+N_2$. We therefore perform a canonical transformation based on the generating function

$$F=\frac{1}{2}(\beta_1-\beta_2)J+\frac{1}{2}(\beta_1+\beta_2)P, \tag{12}$$

yielding

$$N_1=\frac{\partial F}{\partial\beta_1}=\frac{1}{2}(P+J), \quad N_2=\frac{\partial F}{\partial\beta_2}=\frac{1}{2}(P-J), \tag{13}$$

$$\theta_1=\frac{\partial F}{\partial J}=\frac{1}{2}(\beta_1-\beta_2), \quad \theta_2=\frac{\partial F}{\partial P}=\frac{1}{2}(\beta_1+\beta_2). \tag{14}$$

As a result we obtain the reduced three DOF Hamiltonian expressed in the two dimer DOFs $p_{n=1,2},\phi_{n=1,2}$ and an additional J-θ oscillator describing the power (energy) exchange between them

$$\begin{aligned}H(p_1,\phi_1,p_2,\phi_2,J,\theta)&=\frac{\gamma}{4}J^2+\frac{\gamma}{2}p_1^2+\sqrt{\tfrac{1}{4}(P+J)^2-p_1^2}\\&\times\cos(\phi_1)+\frac{\gamma}{2}p_2^2+\sqrt{\tfrac{1}{4}(P-J)^2-p_2^2}\\&\times\cos(\phi_2)+W\sqrt{[\tfrac{1}{2}(P+J)-p_1[\tfrac{1}{2}(P-J)+p_2]}\\&\times\cos[\theta-\tfrac{1}{2}(\phi_1+\phi_2)].\end{aligned} \tag{15}$$

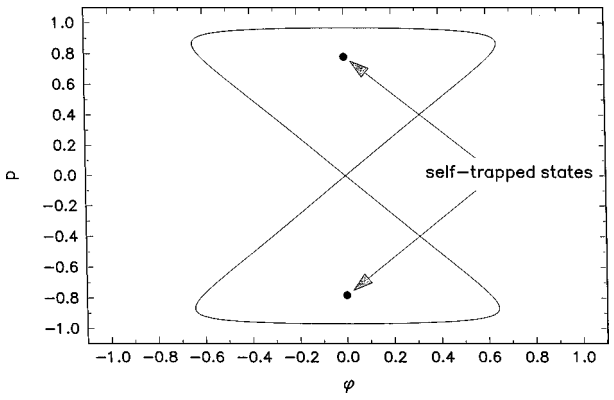

FIG. 1. Phase plane of a DNLS dimer of $\gamma=1.6$ showing the homoclinic structure. The two self-trapped states inside the separatrix are indicated.

We simplified the notation as $\theta_1\rightarrow\theta$ and further dropped a constant contribution from the Hamiltonian because it does not affect the equations of motion.

The integrable equations of motion in the dimer variables $(p_n\equiv p,\phi_n\equiv\phi)$ for an isolated dimer $(W=0)$ are given by

$$\dot{p}=-\sqrt{N^2-p^2}\,\sin\phi, \quad \dot{\phi}=\gamma p-\frac{p}{\sqrt{N^2-p^2}}\cos\phi. \tag{16}$$

For $N\gamma<1$ the system (16) possesses two stable elliptic fixed points located at $(p,\phi)=(0,0)$ and $(p,\phi)=(0,\pm\pi)$, respectively. The corresponding symmetric and asymmetric mode patterns are symbolically expressed as $(\uparrow,\uparrow)$, respectively $(\uparrow,\downarrow)$. For $N\gamma>1$ a bifurcation takes place and the elliptic point at the origin is converted into a hyperbolic fixed point. The hyperbolic point is connected to itself by a pair of homoclinic orbits formed by its coinciding stable and unstable manifolds. Inside each half of the figure-eight separatrix there are elliptic fixed points located at

$$p_e^{\pm}=\pm\sqrt{N^2-1/\gamma^2}, \quad \phi_e=0, \tag{17}$$

which represent stationary self-trapped states. In the upper half plane the latter are assigned to the mode patterns $(\uparrow\uparrow)$, which in the limit of $N\gamma\rightarrow\infty$ yields $(\uparrow.)$. The elliptic-type dynamical rotations around them correspond to one-sided oscillations of the occupation difference, i.e., $p(t)>0$ $[p(t)<0]$ in the upper [lower] part of the homoclinic structure. Finally, for $N\gamma>2$ a further transition occurs where the separatrix embraces also the points $p=\pm N,\phi=0$. As seen from Eq. (17), the limits $N\rightarrow\infty$ and/or $\gamma\rightarrow\infty$ result in strong self-trapping at one of the monomers, i.e., $p\rightarrow\pm N$. Figure 1 shows the homoclinic structure in the p-ϕ phase plane.

B. Solvable configurations and nonlinear modes

There exist special configurations (dependent on the initial conditions) for which the DNLS tetramer can be integrated in closed form. Andersen and Kenkre [40] presented some exact analytical solutions for N-site DNLS systems with localized initial conditions and a class of more general but symmetric initial conditions. We emphasize that our study differs from those of [40] since the initial conditions

leading in our cases to completely solvable tetramer configurations are not included in the discussions in [40]. Moreover, in addition to the symmetric couplings of $V=W$ we cover a more general case allowing also asymmetry in the couplings, viz. $V\neq W$.

We prove that for the mirror symmetric initial conditions $p_1(0)=-p_2(0)$, $\phi_1(0)=-\phi_2(0)$, and $J(0)=0$ as well as $\theta(0)=0$, the tetramer system can be solved exactly. We refer to these solvable cases as a *solvable tetramer configuration* (STC). The system solutions are given by those for two isolated asymmetric dimers and $p_1(t)\equiv -p_2(t)$, $\phi_1(t)\equiv -\phi_2(t)$, and $N_1(t)\equiv N_2(t)\equiv N$ for all times. The system can be solved regardless of the values for coupling strengths V and W.

To show the validity of the above statement regarding the STC we introduce the following symplectic change of variables induced by the generating function:

$$F=\frac{1}{2}(\phi_1+\phi_2)X+\frac{1}{2}(\phi_1-\phi_2)Y, \tag{18}$$

relating the old and new variables as

$$X=p_1+p_2, \quad \Phi=\frac{1}{2}(\phi_1+\phi_2), \tag{19}$$

$$Y=p_1-p_2, \quad \Omega=\frac{1}{2}(\phi_1-\phi_2). \tag{20}$$

The Hamiltonian expressed in the new variables becomes

$$\begin{aligned} H=&\frac{\gamma}{4}(J^2+X^2+Y^2)+\sqrt{(P+J)^2-(X+Y)^2}\,\cos(\Phi+\Omega)\\ &+\sqrt{(P-J)^2-(X-Y)^2}\,\cos(\Phi-\Omega)\\ &+\frac{W}{2}\sqrt{(P-Y)^2-(J-X)^2}\,\cos(\theta-\Phi). \end{aligned} \tag{21}$$

In order to show the validity of the STC we note that the Hamiltonian (21) is invariant under simultaneous reflections according to

$$H(X,\Phi,J,\theta;Y,\Omega)=H(-X,-\Phi,-J,-\theta;Y,\Omega). \tag{22}$$

Since the Hamiltonian H is an even function in the arguments $u=(X,\Phi,J,\theta)$ we obtain that

$$\dot{X}|_{u=0}=-\left.\frac{\partial H}{\partial\Phi}\right|_{u=0}=0, \quad \dot{\Phi}|_{u=0}=\left.\frac{\partial H}{\partial X}\right|_{u=0}=0, \tag{23}$$

$$\dot{J}|_{u=0}=-\left.\frac{\partial H}{\partial\theta}\right|_{u=0}=0, \quad \dot{\theta}|_{u=0}=\left.\frac{\partial H}{\partial J}\right|_{u=0}=0. \tag{24}$$

Therefore, the six-dimensional phase space $\mathcal{M}=(X,\Phi,J,\theta,Y,\Omega)$ spanned by the dynamical variables decomposes into $\mathcal{M}=\mathcal{M}_{Y,\Omega}\oplus\mathcal{M}_u$, $\mathcal{M}_{Y,\Omega}\in R^1\times T^1$, and $\mathcal{M}_u\in R^2\times T^2$, respectively. The subspace $\mathcal{M}_u=(X_0,\Phi_0,J_0,\theta_0)$ contracts to the point (0,0,0,0). The integrable dynamics takes actually place on the two-dimensional subspace $\mathcal{M}_{Y,\Omega}=(Y,\Omega)\in R^1\times T^1$.

In the case of the STC the Hamiltonian $H=H(Y,\Omega;u=0)$ reads

$$H_{Y,\Omega}=\frac{\gamma}{4}Y^2+2\sqrt{P^2-Y^2}\cos(\Omega)+\frac{W}{2}(P-Y). \tag{25}$$

This Hamiltonian describes an asymmetric DNLS dimer system, the solution of which can be expressed via Jacobian and Weierstrassian elliptic functions [41–44].

In the context of the present study, which is to gain insight into the features of localized DNLS modes, we focus interest on tetramer excitations belonging to stationary STC's. The first situation arises from an ensemble of two dimer modes related to the stable elliptic point at $(p,\phi)=(0,\pm\pi)$ yielding the tetramer pattern $(\uparrow,\downarrow,\downarrow,\uparrow)$. This mode realizes the global minimum of the energy. Therefore, the Hamiltonian can be used as a Lyapunov function to establish its stability. Regarding the tetramer as embedded in an extended chain, the stability of the antiphase tetramer configuration means that there exist no staggered localized solutions, which is in contrast to the findings of [13,12]. But of more interest are tetramer modes built up from stationary dimer states associated with stationary solutions from the interior of the homoclinic structure or the hyperbolic equilibrium itself (see Fig. 1). With respect to such solutions we distinguish three tetramer mode patterns that are classified according to the superposition of their different stationary dimer states. First, there is the amplitude pattern of $(\overset{\uparrow}{}\uparrow\uparrow\overset{\uparrow}{})$. In the limit of $N\gamma\to\infty$ the mode becomes $(\overset{\uparrow}{}\ldots\overset{\uparrow}{})$ and we call it the *outer local tetramer mode* (OLTM). Second, we have $(\uparrow\overset{\uparrow}{}\overset{\uparrow}{}\uparrow)$ going for $N\gamma\to\infty$ to the pattern $(.\overset{\uparrow}{}\overset{\uparrow}{}.)$, referred to as *inner local tetramer mode* (ILTM). Finally, there remains the case of equipartition of the tetramer energy, viz., the pattern $(\uparrow\uparrow\uparrow\uparrow)$. In the next subsection we are going to show that a stationary STC may become unstable with respect to any symmetry-breaking perturbation.

C. Symmetry-breaking perturbations and resonance layers

We show that symmetry-breaking perturbations of the STC's can lead to instability in the tetramer dynamics. As symmetry-breaking perturbations we define deviations from the STC such that $u\neq 0$, and they are measured by absolute values of the two pairs of variables $(|X|,|\Phi|)$ and $(|J|,|\theta|)$. For initial conditions leading to a STC or being close to it the motion is associated with a strong coupling resonance determined by

$$\begin{aligned} \dot{\theta}-(\dot{\phi}_1+\dot{\phi}_2)/2=&\frac{1}{2}\gamma(p_1+p_2-J)\\ &+\frac{1}{4}\frac{P+J+2p_1}{\sqrt{\frac{1}{4}(P+J)^2-p_1^2}}\cos(\phi_1)\\ &-\frac{1}{4}\frac{P-J-2p_2}{\sqrt{\frac{1}{4}(P-J)^2-p_2^2}}\cos(\phi_2)=0. \end{aligned} \tag{26}$$

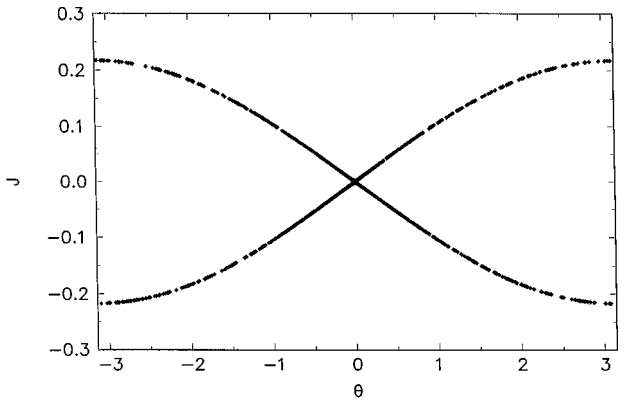

FIG. 2. Master separatrix in the J-θ plane for the coupled dimer-dimer dynamics of $\gamma=1.6$, $P=2$, and $W=0.004$. The initial conditions are $p_1=-0.780\,622\,47$, $p_2=0.780\,622\,79$, $\phi_1=\phi_2=0$, and $J=\theta=0$.

Note that for any STC for which $(J,\theta)=(0,0)$ and $p_1=-p_2, \phi_1=-\phi_2$, the resonance condition (26) is exactly fulfilled. A stability analysis reveals the unstable character of the stationary point $(J,\theta)=(0,0)$ in the J-θ plane. The separatrix assigned to this unstable stationary point develops a stochastic layer due to the nonintegrability of the coupled system. In Fig. 2 we show the separatrix corresponding to the resonance (26) obtained from a numerical integration of the weakly coupled DNLS dimer-dimer system of Eq. (15) with $W=0.004$ projected onto the J-θ phase plane by a time-periodic map. The integration time interval was $0\leqslant t\leqslant 10.000$ and after each time step of $t=50$ a point was set in the J-θ phase plane. The separatrix exhibits a thin stochastic layer. Since the separatrix width determines the maximal amount of energy to be transported from one dimer to the other, we call the J-θ separatrix the *master separatrix*.

Thus perturbations of the STC are connected with dynamics inside the resonance layer and the action J experiences a drift with velocity according to

$$\begin{aligned}\dot{J}&=-(\partial H^1/\partial\theta)\\&=W\sqrt{[\tfrac{1}{2}(P+J)-p_1][\tfrac{1}{2}(P-J)+p_2]}\\&\quad\times\sin[\theta-\tfrac{1}{2}(\phi_1+\phi_2)].\end{aligned}\tag{27}$$

In turn this drift in J changes the energies of the two dimer DOF's due to the dependence $E^0_{1,2}=\gamma p^2_{1,2}+\sqrt{(P\pm J)^2/4-p^2_{1,2}}\cos(\phi_{1,2})$. Therefore, the orbits on the local dimer planes will drift away from their initial positions. The drift in the dimer DOF's initiated and forced by the chaotic layer diffusion of the J action reflects the features of Arnold diffusion [38,45–47].

Concerning the drift motion of action variables inside resonance layers, we exploit now an argumentation of Nekhoroshev [48,49,47]. According to Nekhoroshev, a fast evolution of the action J (with drift velocity of the order of the coupling W) is possible only for resonances and takes place only in directions determined by the resonance vectors. If the unperturbed Hamiltonian is such that the matrix $\partial^2H_0/\partial I^2$ with $I=(p_1,p_2,J)$ is positive (condition of convexity), then it is guaranteed that the evolution extends in a direction leading out of the resonance surface. Hence the resonance gets destroyed and the drift motion of the action appears only for short times so that an exponential bound on the velocity of the action diffusion results [48]. On the other hand, for Hamiltonians for which the convexity is not given one finds on the resonance surface a curve whose tangent at any point lies in the plane spanned by the resonance vector. An action drift with velocity W along this curve suffices that the action variable J shows significant deviations from its initial value already in time intervals of order $1/W$ [48,49].

With respect to the application of the above argumentation to the drift of the action in the stochastic J-θ layer it is now illustrative to inspect the matrix $\partial^2H_0/\partial I^2$, which is given by

$$\begin{pmatrix}\gamma & 0 & D_1\\ 0 & \gamma & D_2\\ D_1 & D_2 & \gamma\end{pmatrix},\tag{28}$$

where

$$D_1\equiv\frac{\partial^2H_0}{\partial p_1\partial J}=\frac{1}{4}\,\frac{p_1\cos(\phi_1)(P+J)}{[\frac{1}{4}(P+J)^2-p_1^2]^{3/2}},\tag{29}$$

$$D_2\equiv\frac{\partial^2H_0}{\partial p_2\partial J}=-\frac{1}{4}\,\frac{p_2\cos(\phi_2)(P-J)}{[\frac{1}{4}(P-J)^2-p_2^2]^{3/2}}.\tag{30}$$

For a comparison of the stability properties of the OLTM and the ILTM we recall that for both modes their two corresponding dimer constituents perform oscillations in the interior of the lobes of their homoclinic structures (see Fig. 1). In both cases the angles are locked in the interval $|\phi_{1,2}|\leqslant\pi/2$ and likewise are the signs of the momenta fixed. Concerning the OLTM characterized by $p_1>0, p_2<0$, the matrix $\partial^2H_0/\partial J^2$ is positive, while for the ILTM of $p_1<0, p_2>0$ it is not. Due to Nekhoroshev we expect for the OLTM only a short time diffusion of the action J, whereas the ILTM may maintain the resonance condition over a long time interval resulting in pronounced action diffusion. Furthermore, from Eq. (27) we see immediately that the drift velocity $\dot{J}$ for an ILTM is larger than for an OLTM.

The findings of the current section lead us to draw the conclusion that the dynamics for initial conditions close to the STC's that is manifested by near-separatrix J-θ motion may become unstable due to diffusion inside the resonance layer. On the other hand, for orbits that remain sufficiently far from the separatrix the evolution is regular. Figure 3 shows the dimer occupation differences $p_{1,2}(t)$ as well as the power exchange variable $J(t)$ for the case of initial conditions sufficiently apart from the unstable point of $(J,\theta)=(0,0)$. Indeed the trajectories exhibit the expected regular behavior. The next section deals with the tetramer dynamics with J-θ initial conditions contained in the stochastic layer around the separatrix for which irregular motion is found.

IV. ENERGY EXCHANGE IN THE COUPLED DIMER-DIMER DYNAMICS

In this section we study the energy exchange dynamics between the two dimeric subunits of the tetramer caused by Arnold diffusion. In Ref. [39] we proved with the help of the Melnikov method the nonintegrability of the DNLS tetramer

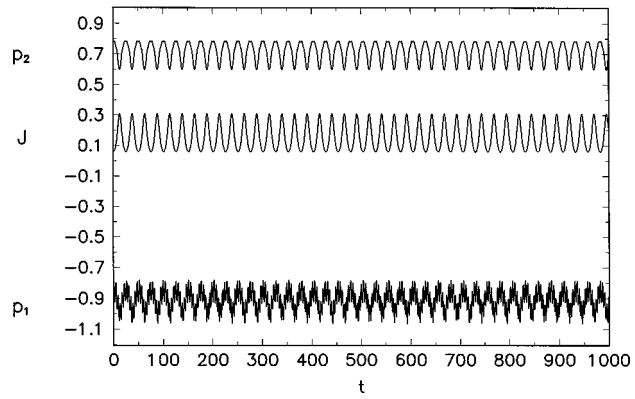

FIG. 3. Evolution of the dimer occupation differences $p_1(t)$ (lowest curve) and $p_2(t)$ (upper curve) and the power difference $J(t)$ (middle curve) for the initial conditions of $p_1=-0.78$, $p_2=0.78$, $J=0.06$, $\phi_1=\phi_2=0$, and $\theta=0$. The parameters are $\gamma=1.6$ and $W=0.01$. The curves reveal regular dynamical behavior.

through the existence of chaotic dynamics supporting the presence of Arnold diffusion. We are interested in tetramer excitations of equal distribution of the conserved tetramer energy between both dimers, i.e., $N_1(0)=N_2(0)$ as well as $E_1^0(0)=E_2^0(0)$. Furthermore, the amplitudes at the opposite sites of the two dimers being the two inner tetramer sites are initially close to a stationary self-trapped state. The situation is described symbolically by the following stationary mode patterns: on dimer 1 ($\uparrow\overset{\uparrow}{\uparrow}$) and on dimer 2 ($\overset{\uparrow}{\uparrow}\uparrow$). To this end we concentrate on initial excitations of the dimers according to $p_1(t)\approx -p_2(t)$ with $|p_{1,2}(t)-p_e^{\mp}|\ll 1$ and $\phi_1(t)\approx -\phi_2(t)$, while $|\phi_{1,2}(t)|\ll 1$. We remark that these initial conditions involve small deviations from the symmetry of the ILTM.

Note that for vanishing coupling $W=0$ the decoupled dimers are each for itself integrable. In particular, the separate dimer energies are both conserved and hence a self-trapped state can never be left. However, when the two dimers become coupled energy migration between them is possible. There arises at least one interesting question to be answered namely, whether this initial excitation pattern of self-trapped amplitudes on the two dimers remains stable under the dimer-dimer interaction or, if not, can there exist any localized structure on the tetramer at all?

The coupled dynamics of the three DOF Hamiltonian dimer-dimer system evolves in the six-dimensional phase space on a five-dimensional energy manifold, which, however, as a whole, is difficult to visualize appropriately. For a geometrical illustration of the complex diffusion process in terms of the dynamics in phase space we invoke therefore projections on the local phase spaces attributed to each single DOF. These three local phase spaces are the two dimer phase planes parametrized in the corresponding p_n-ϕ_n variables ($n=1,2$) and the J-θ phase plane. The local projection method enables us to monitor the actual dynamical state of each subsystem. The sum of these three local pictures contains the complete information about the coupled systems dynamics. For example, the above-described initial conditions are manifested as follows in the local subspaces: In the local dimer phase space of the first dimer, i.e., the p_1-ϕ_1 variable, the initial conditions coincide with a stationary self-trapped state in the lower half plane of $p_1<0$. For the second dimer the initial condition is chosen as a point on a curve encircling closely the elliptic fixed points in the upper half plane ($p_2>0$) inside one-half of the corresponding local figure-eight separatrix. The initial equal distribution of the energy among the dimers is represented in the J-θ plane by the hyperbolic fixed point at (0,0).

In the following we describe the successive stages of the energy exchange dynamics of the coupled dimer-dimer system by focusing on the typical dynamics observed in each of the local phase spaces. We start with the J-θ phase plane as the local phase space describing the power (energy) balance between the two dimers. The chaotic dynamics in the stochastic layer around the master separatrix induces diffusive motion. Therefore, the stochastic layer of the master separatrix guides the action diffusion. Apparently, the larger the possible $J=N_1-N_2$ excursion across the layer the more pronounced the dynamical changes of the local amounts of the dimer powers N_1 and N_2. When diffusing across the J-θ stochastic layer away from the initial point (0,0) into the upper (lower) half-plane of $J>0$ ($J<0$) the local energy of the first dimer increases (diminishes), while that of the second dimer diminishes (increases). In turn these directed changes in the local dimer energies are reflected on the associated dimer phase planes by diffusive motion of the dimer variables (p_n, ϕ_n), $n=1,2$. The diffusive motion in the dimer subplanes initiated and forced by the chaotic diffusion in the stochastic layer in the J-θ plane is characteristic for Arnold diffusion [45,38].

In Fig. 4 we illustrate the dynamics of the energy exchange between the two dimers for a coupling strength $W=0.01$. Projections on the individual subplanes were achieved by a time-periodic map, that is, after a time step of $t=50$ the dynamical state of the subsystem was set as a point in the corresponding plane. Figure 4(a) shows the corresponding J-θ phase plane exhibiting a chaotic layer around the destroyed separatrix in which the action J diffuses. The time evolution of the action $J(t)$ is depicted in Fig. 4(b). Clearly visible is the pronounced diffusive growth from $J=0$ to $J\simeq 0.5$ taking place in the time interval of $0\leqslant t<4800$. The exclusively positive J amplitude performs ''everlasting'' small oscillations around a mean value of $J\simeq 0.5$ to be seen on the corresponding J-θ plane as a horizontal motion [Fig. 4(c)]. This means that the major amount of power $N_1\simeq 5/4$ is then contained in the first dimer, whereas the rest of power (energy) $N_2=P-N_1\simeq 3/4$ remains in the second dimer. The process of directed energy transfer from dimer 1 into dimer 2 becomes transparent in the $p_{1,2}$-$\phi_{1,2}$ planes that we superimposed onto one plane in Fig. 4(d). We show the initial stage of the dynamics up to a time of $t=4000$ when the energy migration takes place. Interestingly, the directed redistribution of major parts of the conserved tetramer energy into one of its dimer components causes enhanced self-trapping of the energy on the corresponding right monomer of the first dimer to be seen in Figs. 4(e) and 4(f), where we plotted the dimer occupation differences $p_1(t)$ and $p_2(t)$, respectively. While on dimer 1 a self-trapped state has been formed with strong localization of the local energy at its right dimer site, the dynamics on dimer 2 is characterized by randomization of the energy over its two monomers [see Fig. 4(f)]. The latter effect of energy equi-

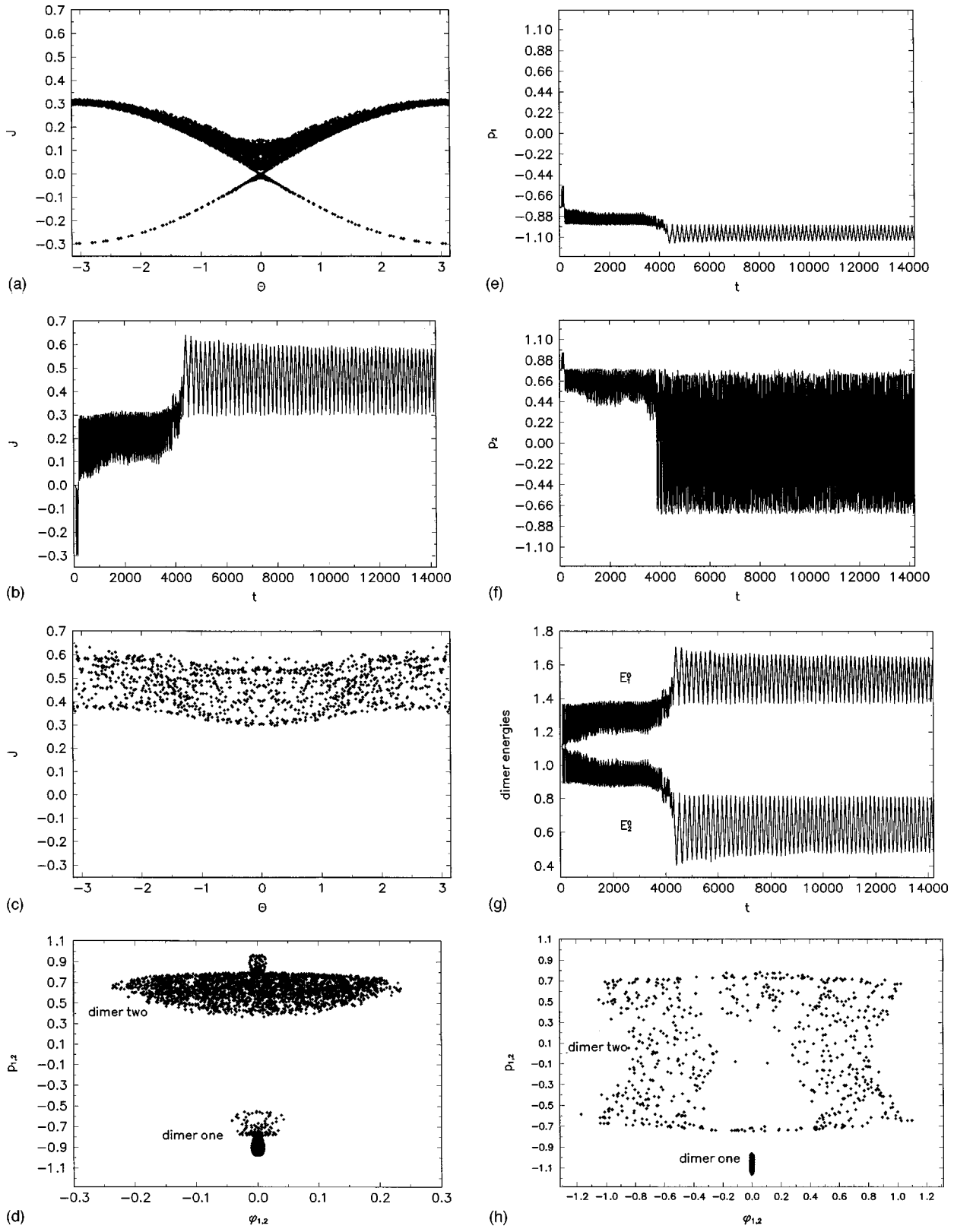

FIG. 4. Dynamics of the energy exchange between two coupled DNLS dimers. The parameters and initial conditions are as in Fig. 1, except for the coupling strength of $W=0.01$. (a) The J-θ plane for $t<4000$. The separatrix exhibits a chaotic layer. (b) Time evolution of $J(t)$. (c) The J-θ plane for $t>4000$. (d) The superimposed phase planes of dimers 1 and 2, respectively, for $0\leqslant t\leqslant 4000$. (e) Dimer occupation difference $p_1(t)$. (f) Dimer occupation difference $p_2(t)$. (g) The evolution of the dimer energies $E^0_{1,2}(t)$ illustrating the directed flow of energy from dimer 2 into dimer 1. (h) The superimposed phase planes of dimers 1 and 2, respectively. For $t>4800$ the final stage of the dynamics of dimer 2 takes place as chaotic motion in the stochastic layer of the separatrix, whereas for dimer 1 the elliptic equilibrium in the lower half plane is encircled.

partition is the result of the chaotic movement of $p_2(t)$ around the value of zero due to nearby separatrix motion on the p_2-ϕ_2 phase plane. The time evolution of the dimer energies $E^0_{1,2}(t)$ in Fig. 4(g) shows the migration of the energy from the second dimer into the first dimer. In Fig. 4(h) we illustrate on the two superimposed dimer subplanes the final stage of the dynamics for $t>4000$, that is, after the energy migration from dimer 2 to dimer 1 has been finished. In Fig. 4(h) one clearly sees that the localized single-site state is characterized by small-amplitude oscillations around an elliptic fixed point in the p_1-ϕ_1 subplane.

We emphasize that in the final stage the dynamics in the p_2-ϕ_2 subsystem takes place as diffusion inside a thick stochastic layer. The thick stochastic layers form the dominant part of the Arnold web containing the thin layers of many other resonances too. As a hallmark of Arnold diffusion the dynamics preferably takes place in thick stochastic layers [45,38]. In this way the thick layer p_2-ϕ_2 motion in the separatrix of the unstable equilibrium is maintained and there will no pathway back leding to even the vicinity of the starting point at the self-trapped state belonging to the stable $p_{1,2}$-$\phi_{1,2}$ equilibria. Consequently, the coupled dimer-dimer motion will hardly return to the initial state of energy equipartition and hence the energy transfer from one dimer into the other is *irreversible*. In conclusion, a long-lived single-site localized state on the first dimer is observed storing the majority of the energy in it, whereas on the second dimer the remaining little energy is randomized over its two sites.

To summarize, we have seen that in the case of a weakly coupled dimer-dimer system the formation of a specific localized mode excitation pattern with energy localization at a single site is possible. This localized state has emerged from a situation of initial equal energy distribution among the two dimer subunits with an amplitude pattern close to an inner local tetramer mode, that is, $(\uparrow\hat{\uparrow}\hat{\uparrow}\uparrow)$. The directed energy migration results eventually in a single-site self-trapped state on only one of the dimers according to the mode pattern $(\uparrow\uparrow\hat{\uparrow}\uparrow)$. This long-lived and stable localized state shows the typical features of a stationary solitarylike excitation or intrinsically localized mode.

We investigated also the dynamics corresponding to initial conditions close to the outer local tetramer mode, viz., $(\hat{\uparrow}\uparrow\uparrow\hat{\uparrow})$. It turns out that it is robust under weak symmetry-breaking perturbations maintaining its excitation pattern. The findings are summarized in Fig. 5.

V. STABILITY PROPERTIES OF THE EVEN- AND ODD-PARITY LOCALIZED MODES

In this section we consider localized excitation patterns of an extended DNLS lattice chain. When we view the tetramer system as a four-site element embedded in a longer (infinite) lattice chain we can exploit the results of the above-performed tetramer stability discussions for interpreting them in the context of strongly localized modes on the extended chain. In particular we see that the mirror-symmetric tetramer initial conditions close to an ILTM resemble the excitation pattern of the central four-site element for the strongly localized even-parity mode on an extended DNLS chain, viz., $(\ldots\uparrow\hat{\uparrow}\hat{\uparrow}\uparrow\ldots)$.

In adopting the results reported in the preceding section

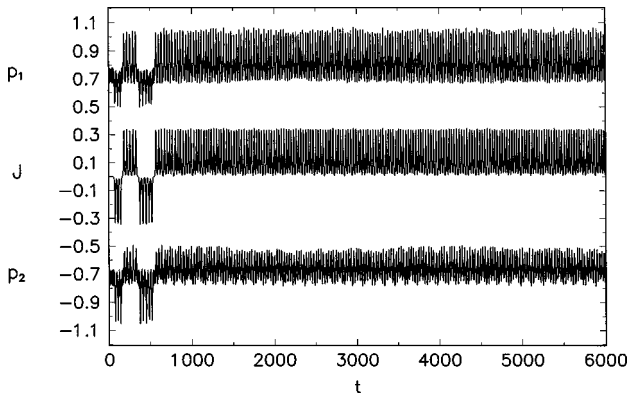

FIG. 5. Stability of the OLTM. The initial conditions are as in Fig. 1, except for the sign change of p_1 to 0.780 622 47 and p_2 to $-0.780\,624\,79$. The dimer-dimer coupling is taken as $W=0.1$ which is 10 times larger than the one used for the ILTM of Fig. 4.

for the localized structure formation on the tetramer to extended lattice dynamics we anticipate that the perturbed even-parity mode collapses to the odd-parity mode characterized by the stationary mode pattern $(\ldots\uparrow\hat{\uparrow}\uparrow\ldots)$. This prediction was confirmed in our numerical studies. Figure 6 shows the evolution of the amplitude profiles for a DNLS chain with open boundaries. We excited initially two adjacent lattice sites corresponding to a very strong localized even-parity mode. A symmetry-breaking perturbation was imposed through small difference in the two excited amplitudes of the order of 10^{-5}. After a short transient time of phonon emission from the excitation peak into extended parts of the lattice one clearly sees the two-site excitation pattern collapsing to a single-site state representing the stationary odd-parity mode.

Our result is in qualitative agreement with the findings of Laedke, Spatschek, and Turitsyn [50] in their study of a DNLS with a tunable power nonlinearity. They showed that unstable discrete solitons centered between two lattice sites (even-parity modes) collapse eventually into more stable intrinsically localized modes. For a nonlinearity power larger than our cubic one this final state is a time-dependent local-

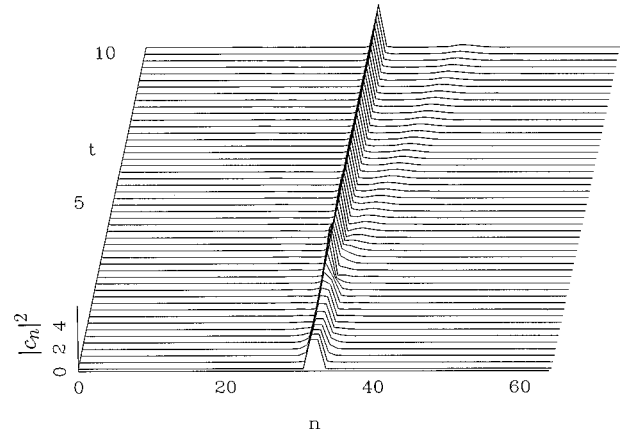

FIG. 6. Amplitude profile on an extended DNLS chain illustrating the intrinsic collapse of the initially excited even-parity mode to the odd-parity one. The parameters are $P=8$ and $\gamma=V=1$. The initial difference in the amplitude of the two excited lattice sites is 10^{-5}.

ized mode corresponding to an *oscillating two-soliton state* [50]. With the present study for cubic nonlinearities we demonstrate that the fate of the perturbed even-parity mode is to collapse to a *standing* solitonlike state that is, however, nonoscillating. Kivshar and Campbell [13] argued that the even-parity and odd-parity stationary DNLS modes can be viewed as two different states of the same localized state, but at different fixed instants in time. In more detail, while moving the localized state rigidly through the lattice it has its center at a certain time at a lattice site (odd-parity mode), whereas at another time it will be centered between two sites (even-parity mode). From a comparison of the corresponding mode energies one can also infer the stability properties. The odd-parity mode has lower energy than the even-parity one. Thus the latter shows an instability [13]. We underline that our analysis goes beyond the one performed in [13] because it is not restricted to a stationary analysis of DNLS modes. Moreover, we reveal in detail the *dynamical* instability of the even-parity mode entailing an intrinsic dynamical collapse to the odd-parity mode.

Contrary to the even-parity mode, the odd-parity mode remains stable with respect to symmetry perturbations. In order to explain the stability of the odd-parity mode we can invoke again a local phase-space picture. Since effectively only three lattice oscillators are involved in its excitation pattern the local phase space this time belongs to the central trimer segment truncated from the extended chain. The perfect excitation pattern of the odd-parity mode ($\uparrow\hat{\uparrow}\uparrow$) yields integrable trimer motion. By means of a Poincaré map it can be shown that this stationary mode pattern is represented by an elliptic fixed point on the corresponding cross section. Symmetry-breaking perturbations of the odd-parity mode produce a stability island of the Poincaré map for which integrable quasiperiodic motion surrounds the elliptic fixed point. This offers an explanation for the robustness of the odd-parity mode with respect to perturbations in terms of the local trimer phase-space dynamics. In summary we see that unlike the even-parity mode, which even under small breaking of its symmetry is readily destroyed, the odd-parity mode persists for a rather strong breaking of its symmetry pattern.

VI. SUMMARY

We have studied the energy transfer along a DNLS lattice chain. As a first step we showed that a resonant finite element can be decoupled from the lattice. In the first part of the paper a four-element segment, i.e., a DNLS tetramer, was investigated. We identified certain initial conditions for which the tetramer system can be solved exactly. For two weakly coupled dimers the persistence of their stationary dimer modes as tetramer modes was investigated. It was shown that perturbations of the tetramer modes exhibiting self-trapped amplitudes at the two inner tetramer sites (inner local tetramer modes) lead to unstable motion. The energy migration along the tetramer was studied numerically. In particular, imposing perturbations on the excited inner local tetramer mode, chaotic dynamics inside resonance layers was found and diffusion of an action variable expressing the energy sharing between the dimers appeared. Due to the action diffusion, a directed and irreversible energy flow from one dimer into the other takes place. As an interesting phenomenon one observes finally the creation of a coherent structure in the form of a large-amplitude state localized at a single site of the tetramer. This localized state is dynamically stable. The tetramer results are applicable to the search for localized vibrational modes in molecular tetramer studies, but are also of interest in nonlinear optics when arrays of four coupled waveguides are considered.

In the second part of the paper we focused interest on the energy exchange dynamics along an extended DNLS chain. Attention was paid to the occurrence of localized stationary modes, that is, the odd-parity and even-parity modes, respectively. To relate the tetramer results obtained in the first part of the paper to the studies of dynamics on the extended lattice we used that the main excitation pattern of the even-parity mode on the extended lattice is localized at only four lattice elements and its shape resembles an inner local tetramer mode. Therefore, the tetramer studies can serve as a four-element approximation of the extended lattice dynamics. Especially from the instability of the inner local tetramer mode, one can predict a decay of the even-parity mode. Moreover, the above-reported creation of the single-site localized tetramer state corresponds on the extended lattice to the formation of the odd-parity mode. In the numerical study of the extended DNLS lattice we have observed indeed an intrinsic collapse of the initially excited even-parity mode to the odd-parity one. Thus we have been able to demonstrate that the most stable localized excitation of a DNLS chain is provided by a one-site breather. This result is of importance for applications of the DNLS equation in describing arrays of nonlinear optical waveguides since it shows what type of excitation can be stored in the array in a reliable and stable way. With regard to applications of DNLS modeling larger molecular systems such as globular protein chains or crystalline acetanilide, our results show that self-trapping of vibrational energy occurs preferably on only one subunit of the chain.

ACKNOWLEDGMENT

This work was supported by the Deutsche Forschungsgemeinschaft via Sonderforschungsbereich 337.

[1] J.C. Eilbeck, P.S. Lomdahl, and A.C. Scott, Physica D **16**, 318 (1985).

[2] T. Holstein, Ann. Phys. (N.Y.) **8**, 325 (1959); V.M. Kenkre and D.K. Campbell, Phys. Rev. **34**, 4595 (1986); A.S. Davydov and N.I. Kislukha, Phys. Status Solidi B **59**, 465 (1973); N. Finlayson and G.I. Stegeman, Appl. Phys. Lett. **56**, 2276 (1990); Y. Chen, A.W. Snyder, and D.J. Mitchell, Electron. Lett. **26**, 77 (1990); M.I. Molina, W.D. Deering, and G.P. Tsironis, Physica D **66**, 135 (1993); H. Feddersen, P.L. Christiansen, and M. Salerno, Phys. Scr. **43**, 353 (1991); L.J. Bernstein, Opt. Commun. **94**, 406 (1992); D. Hennig, Physica D **64**, 121 (1993).

[3] A.C. Scott, I.J. Bigio, and C.T. Johnston, Phys. Rev. B **39**, 12 883 (1989).
[4] H. Feddersen, Phys. Lett. A **154**, 391 (1991).
[5] L.D. Faddeev and L.A. Takhtajan, *Hamiltonian Methods in the Theory of Solitons* (Springer-Verlag, Berlin, 1987).
[6] M. J. Ablowitz and P. A. Clarkson, *Solitons, Nonlinear Evolvlution Equations and Inverse Scattering* (Cambridge University Press, New York, 1991).
[7] M. Toda, J. Phys. Soc. Jpn. **22**, 431 (1975).
[8] M. J. Ablowitz and J. F. Ladik, J. Math. Phys. (N.Y.) **17**, 1011 (1976).
[9] B.M. Herbst and M.J. Ablowitz, Phys. Rev. Lett. **62**, 2065 (1989).
[10] R. Scharf and A.R. Bishop, **43**, 6535 (1991).
[11] S. Takeno, J. Phys. Soc. Jpn. **58**, 759 (1989).
[12] D. Cai, A.R. Bishop and N. Grønbech Jensen, Phys. Rev. Lett. **72**, 591 (1994).
[13] Yu.S. Kivshar and D.K. Campbell, Phys. Rev. E **48**, 3077 (1993).
[14] Yu.S. Kivshar, Phys. Lett. A **161**, 80 (1991).
[15] Yu.S. Kivshar and M. Peyrard, Phys. Rev. A **46**, 3198 (1992).
[16] D.K. Campbell and M. Peyrard, in *Chaos*, edited by D.K Campbell (American Institute of Physics, New York, 1990), p. 305.
[17] A.J. Sievers and S. Takeno, Phys. Rev. Lett. **61**, 970 (1988).
[18] J.B. Page, Phys. Rev. B **41**, 7835 (1990).
[19] S. Takeno and S. Homma, J. Phys. Soc. Jpn. **60**, 731 (1991); **62**, 835 (1993); S. Takeno, *ibid.* **61**, 2821 (1992); S.R. Bickham, S.A. Kiselev, and A.J. Sievers, Phys. Rev. B **47**, 14 206 (1993).
[20] T. Dauxois, M. Peyrard, and C.R. Willis, Physica D **57**, 267 (1992); Phys. Rev. E **48**, 4768 (1993); T. Dauxois and M. Peyrard, Phys. Rev. Lett. **70**, 3935 (1993).
[21] Yu.S. Kivshar, Phys. Rev. E **48**, 4132 (1993).
[22] S. Flach, C.R. Willis, and E. Olbrich, Phys. Rev. E **49**, 836 (1994); S. Flach and C.R. Willis, Phys. Lett. A **181**, 232 (1993); Phys. Rev. Lett. **72**, 1777 (1994).
[23] S. Flach, Phys. Rev. E **50**, 3134 (1994); **51**, 1503 (1995); **51**, 3579 (1995).
[24] Ch. Claude, Yu.S. Kivshar, K.H. Spatschek, and O. Kluth, Phys. Rev. B **47**, 14 228 (1992).
[25] R.S. MacKay and S. Aubry, Nonlinearity **7**, 1623 (1994).
[26] S. Aubry, Physica D **86**, 284 (1995).
[27] S. Takeno and M. Peyrard, Physica D **92**, 140 (1996).
[28] P. Marquié, J.M. Bilbault, and M. Remoissenet, Phys. Rev. E **51**, 6127 (1995).
[29] G.P. Tsironis and S. Aubry, Phys. Rev. Lett. **77**, 5225 (1996).
[30] K.W. Sandudsky, J.B. Page, and K.E. Schmidt, Phys. Rev. B **46**, 6161 (1992).
[31] A.B. Aceves, C. De Angelis, S. Trillo, and S. Wabnitz, Opt. Lett. **19**, 332 (1994); A.B. Aceves, C. De Angelis, A.M. Rubenchik, and S.K. Turitsyn, *ibid.* **19**, 329 (1994).
[32] A.B. Aceves, C. De Angelis, T. Peschel, R. Muschall, F. Lederer, S. Trillo, and S. Wabnitz, Phys. Rev. E **53**, 1172 (1995).
[33] G. Benettin, L. Galgani, and A. Giogilli, Nuovo Cimento **89**, 89 (1985).
[34] G. Benettin, L. Galgani, and A. Giogilli, Nuovo Cimento **89**, 103 (1985).
[35] A. Osuka, K. Marnyama, and I. Yamzaki, Chem. Phys. Lett. **165**, 392 (1990).
[36] U. Rempel, B. von Maltzan, and C. Borczyskowski, Chem. Phys. Lett. **165**, 489 (1990).
[37] B.M. Pierce, in *Davydov's Solitons Revisited*, Vol. 243 of *NATO Advanced Study Institute, Series B: Physics*, edited by P.L. Christiansen and A.C. Scott (Plenum, New York, 1991).
[38] A.J. Lichtenberg and M.A. Liebermann, *Regular and Stochastic Motion* (Springer-Verlag, New York, 1992).
[39] D. Hennig and H. Gabriel, J. Phys. A **28**, 3749 (1995).
[40] J.D. Andersen and V.M. Kenkre, Phys. Rev. B **47**, 11 134 (1993); Phys. Status Solidi B **177**, 397 (1993).
[41] A.C. Scott, Phys. Scr. **42**, 14 (1990).
[42] B. Esser and D. Hennig, Z. Phys. B **83**, 285 (1991).
[43] V. Szöcs and P. Banacky, Phys. Rev. A **45**, 5415 (1992).
[44] G.P. Tsironis, Phys. Lett. A **173**, 381 (1993).
[45] V.I. Arnold, *Mathematical Methods of Classical Mechanics* (Springer-Verlag, New York, 1978).
[46] V.I. Arnold, Sov. Math. Dokl. **5**, 581 (1964).
[47] B.V. Chirikov, Phys. Rep. **52**, 263 (1979).
[48] N.N. Nekhoroshev, Russ. Math. Surveys **32**, 1 (1977); Trudy Sem. Petrovs. **5**, 5 (1979).
[49] V.I. Arnold *Geometrical Methods in the Theory of Ordinary Differential Equations* (Springer-Verlag, New York, 1988).
[50] E.W. Laedke, K.H. Spatsckek, and S.K. Turitsyn, Phys. Rev. Lett. **73**, 1055 (1994).